

# Roles of isoscalar hyperons in probing the density dependence of the nuclear symmetry energy

W. Z. Jiang\*

Shanghai Institute of Applied Physics,  
Chinese Academy of Sciences, Shanghai 201800, China

## Abstract

The role of the isoscalar hyperon  $\Lambda$  in probing the density dependence of the nuclear symmetry energy is studied in multi- $\Lambda$  hypernuclei, hyperon-rich matter and neutron stars in relativistic models. Relationships between the properties of three types of objects and the neutron thickness in  $^{208}\text{Pb}$  are established with respect to the isoscalar-isovector coupling that modifies the density dependence of the symmetry energy. The exotic isotopes far from the neutron drip line can be stabilized by filling in considerable  $\Lambda$  hyperons. The difference of the binding energy of multi- $\Lambda$  hypernuclei from different models is attributed to different symmetry energies. The isovector potential together with the neutron thickness in multi- $\Lambda$  hypernuclei investigated is very sensitive to the isoscalar-isovector coupling. The large sensitivity of the  $\Lambda$  hyperon fraction to the isoscalar-isovector coupling occurs at about  $2 \sim 3\rho_0$  in beta equilibrated hyperon-rich matter. In neutron stars with hyperonization, an on-off effect with respect to the isoscalar-isovector coupling exists for the neutron star radius.

PACS: 21.60.-n, 21.80.+a, 26.60.+c, 27.60.+j

Keywords: Hypernuclei, bulk matter, neutron stars, relativistic mean field model

---

\*Email: jiangwz02@hotmail.com, Also at Center of Theoretical Nuclear Physics, National Laboratory of Heavy Ion Accelerator, Lanzhou 730000, China

The symmetry energy is pervasively related to the descriptions of nuclear structures and reactions in laboratories and astrophysics[1, 2, 3]. However, the density dependence of the symmetric energy is still poorly known[4, 5] to date. Therefore, theoretical uncertainties exist in the understanding of a large number of properties of neutron stars and heavy nuclei[6, 7], nuclei far from the  $\beta$  stability[8, 9, 10], heavy ion collisions[5, 11] and consequently probable hadron-quark phase transition[12], etc. Many factors that influence the isovector potential directly or indirectly can modify the behavior of the density dependence of the symmetry energy. Recently the density dependence of the symmetry energy has been extensively explored through the inclusion of the isoscalar-isovector coupling terms in relativistic mean field (RMF) models[6, 7, 8, 13]. These new terms enable one modify the neutron skin of heavy nuclei without changing the charge radius and a variety of ground-state properties that are well constrained experimentally. On the other hand, the charge density distributions for some light exotic nuclei near drip lines that are not determined yet are sensitive to the isoscalar-isovector couplings[10, 14].

Hypernuclei that are produced through strangeness transfer reactions mostly contain only one hyperon, and just a few double  $\Lambda$  hypernuclear events were observed[15, 16, 17]. Through heavy-ion collisions it may possibly create an environment which is favorable to the formation of metastable exotic multihypernuclear objects (MEMOs) such as multi- $\Lambda$  hypernuclei. Schaffner et.al. showed that multi- $\Lambda$  hypernuclei were more strongly bound than normal nuclei using the RMF model[18, 19]. Recently, Jevorsek et.al. set limits on the existence and properties of exotic objects such as strangelets and MEMOs, and provided limits as low as  $10^{-7}$  for  $M/Z$  up to 120 through a reanalysis of related data[20]. In bulk matter, strangeness can be formed by virtue of the strong interaction, and hyperons may be important constituents of neutron stars. Many important effects of hyperonization in neutron stars have been found in the past (for a review, see[21]). For instance, hyperonization reduces the maximum mass of neutron stars as much as  $3/4M_{\odot}$ [22, 23]. Schaffner et.al. found that a phase transition to hyperon matter may even possibly occur in neutron stars[24]. In this work, it is the aim to constrain the density dependence of the symmetry energy through the investigation of properties of multi- $\Lambda$  hypernuclei, hyperon-rich matter and neutron stars with hyperonization. We will perform the investigation in RMF models considering the isoscalar-isovector coupling terms that soften the symmetry energy at large densities.

The modification in MEMOs and hyperon-rich matter due to the isoscalar-isovector couplings is usually considered to be small due to the relatively weak meson-hyperon coupling. As pointed out in Refs.[18, 19] that the MEMOs may reach a very high baryon density ( $2.5 \sim 3\rho_0$ ) like strangelets. In hyperon-rich matter, the appearance of  $\Lambda$  hyperons occurs at about twice normal density. Since the higher density relates to the larger isoscalar potentials (or fields), the isoscalar-isovector couplings will induce large modifications. In hyperon-rich matter, we will focus on the relation between the  $\Lambda$  fraction and the isoscalar-isovector coupling. As the determination of properties of neutron stars with hyperonization needs the equation of state of hyperon-rich matter, we may search for the observable consequence relating to the density dependence of the symmetry energy. As examples of MEMOs, we will consider multi- $\Lambda$  hypernuclei based on the Ca isotope far off the normal neutron drip line at the fixed isospin. In this way, we can observe the extension of the drip line, and explore the density dependence of the symmetry energy by shifting the isoscalar field.

In this study, additional strange mesons  $\sigma^*$  (i.e.  $f_0$ , 975MeV) and  $\phi$  (1020MeV) are also included in RMF models to describe the strong  $\Lambda\Lambda$  attraction as in Refs.[19, 24, 25]. The effective Lagrangian density is given as follows

$$\begin{aligned}
\mathcal{L} = & \bar{\psi}_B [i\gamma_\mu \partial^\mu - M_B + g_{\sigma B} \sigma - g_{\omega B} \gamma_\mu \omega^\mu - g_{\rho B} \gamma_\mu \tau_3 b_0^\mu \\
& + \frac{f_{\omega B}}{2M_N} \sigma_{\mu\nu} \partial^\nu \omega_0^\mu - e \frac{1}{2} (1 + \tau_c) \gamma_\mu A^\mu] \psi_B - U(\sigma, \omega^\mu, b_0^\mu) \\
& + \frac{1}{2} (\partial_\mu \sigma \partial^\mu \sigma - m_\sigma^2 \sigma^2) - \frac{1}{4} F_{\mu\nu} F^{\mu\nu} + \frac{1}{2} m_\omega^2 \omega_\mu \omega^\mu \\
& - \frac{1}{4} B_{\mu\nu} B^{\mu\nu} + \frac{1}{2} m_\rho^2 b_{0\mu} b_0^\mu - \frac{1}{4} A_{\mu\nu} A^{\mu\nu} + \mathcal{L}_Y
\end{aligned} \tag{1}$$

and  $\mathcal{L}_Y$  is for the strange meson-hyperon interactions and free fields of strange mesons

$$\begin{aligned}
\mathcal{L}_Y = & \bar{\psi}_Y [g_{\sigma^* Y} \sigma^* - g_{\phi Y} \gamma_\mu \phi^\mu] \psi_Y + \frac{1}{2} (\partial_\mu \sigma^* \partial^\mu \sigma^* - m_{\sigma^*}^2 \sigma^{*2}) \\
& - \frac{1}{4} (\partial^\mu \phi^\nu - \partial^\nu \phi^\mu) (\partial_\mu \phi_\nu - \partial_\nu \phi_\mu) + \frac{1}{2} m_\phi^2 \phi_\mu \phi^\mu
\end{aligned} \tag{2}$$

where  $\psi_B$ ,  $\sigma$ ,  $\omega$ , and  $b_0$  are the fields of the baryon, scalar, vector, and charge-neutral isovector-vector mesons, with their masses  $M_B$ ,  $m_\sigma$ ,  $m_\omega$ , and  $m_\rho$ , respectively.  $A_\mu$  is the field of the photon.  $g_{iB}$  ( $i = \sigma, \omega, \rho$ ) and  $f_{\omega B}$  are the corresponding meson-baryon couplings.  $\tau_3$  is the third component of isospin Pauli matrix for nucleons and  $\tau_3 = 0$  for the  $\Lambda$  hyperon.  $\tau_c$  is a constant relating to the baryon charge.  $F_{\mu\nu}$ ,  $B_{\mu\nu}$ , and  $A_{\mu\nu}$  are the strength tensors of the  $\omega$ ,

$\rho$  mesons and the photon, respectively

$$F_{\mu\nu} = \partial_\mu\omega_\nu - \partial_\nu\omega_\mu, \quad B_{\mu\nu} = \partial_\mu b_{0\nu} - \partial_\nu b_{0\mu}, \quad A_{\mu\nu} = \partial_\mu A_\nu - \partial_\nu A_\mu \quad (3)$$

The self-interacting terms of  $\sigma, \omega$ -mesons and the isoscalar-isovector ones are in the following

$$U(\sigma, \omega^\mu, b_0^\mu) = \frac{1}{3}g_2\sigma^3 + \frac{1}{4}g_3\sigma^4 - \frac{1}{4}c_3(\omega_\mu\omega^\mu)^2 - 4g_{\rho N}^2(\Lambda_s g_{\sigma N}^2\sigma^2 + \Lambda_v g_{\omega N}^2\omega_\mu\omega^\mu)b_{0\mu}b_0^\mu \quad (4)$$

For the hyperon-rich matter, the chemical equilibration is established on weak interactions of baryons and leptons as in Ref.[22, 26]. We study chemically equilibrated and charge neutral hyperon-rich matter including baryons ( $N, \Lambda, \Xi$ ) and leptons ( $e, \mu$ ) without  $\Sigma$  hyperons, since  $\Sigma$  hyperons do not appear[24, 25] according to the fact that the isoscalar potential changes sign in the nuclear interior and becomes repulsive based on recent  $\Sigma^-$  atomic data [27]. For the finite system, we consider the spherical case. The solution detail can be referred to Refs.[28, 29], and it is not repeated here. The pairing correlation of nucleons in nuclei is considered in the BCS approximation as in Refs.[14].

We perform calculations with the NL3 [30] and S271[6] parameter sets. These two models share the same binding energy per nucleon (16.24MeV) and incompressibility (271MeV) at the same Fermi momentum  $k_F = 1.30\text{fm}^{-1}$  ( $\rho_0 = 0.148\text{fm}^{-3}$ ). The symmetry energy is given by[7]

$$a_4 = \frac{k_F^2}{6E_F^*} + \frac{g_\rho^2}{3\pi^2} \frac{k_F^3}{m_\rho^{*2}} \quad (5)$$

with  $E_F^* = \sqrt{k_F^2 + M_N^{*2}}$  and  $m_\rho^{*2} = m_\rho^2 + 8g_{\rho N}^2(g_{\sigma N}^2\Lambda_s\sigma^2 + g_{\omega N}^2\Lambda_v\omega_0^2)$ . The density dependence of the symmetry energy is different between two models because of different  $g_{\rho N}$ ,  $m_\rho^*$  and  $M_N^*$  ( $M_N^* = 0.59M_N$  for the NL3 and  $M_N^* = 0.7M_N$  for the S271).

The  $\omega$  and  $\rho$  meson couplings to the hyperons are given by the SU(3) relations:  $g_{\omega\Lambda} = 2/3g_{\omega N} = 2g_{\omega\Xi}$ ,  $g_{\rho\Lambda} = 0$  and  $g_{\rho\Xi} = g_{\rho N}$ . The  $\sigma$  meson coupling to the hyperons is determined by reasonable hyperon potentials in nuclear matter:  $U_\Lambda^{(N)} = -30\text{MeV}$  and  $U_\Xi^{(N)} = -20\text{MeV}$ . The coupling constants  $g_{\phi\Lambda}$  and  $g_{\phi\Xi}$  are taken to satisfy the SU(6) relation:  $g_{\phi\Xi}/g_{\omega N} = 2g_{\phi\Lambda}/g_{\omega N} = -2\sqrt{2}/3$ , and the  $g_{\sigma^*\Lambda}$  is fitted to improve the  $\Lambda\Lambda$  interaction matrix element  $\Delta B_{\Lambda\Lambda}$ [19]. In Ref.[24], the  $g_{\sigma^*\Lambda}$  is taken in a range close to the  $g_{\sigma N}$ . We take the ratio of the scalar coupling constant to be  $g_{\sigma^*\Lambda}/g_{\sigma N} = 0.76$  in NL3 with a potential for the  $\Lambda$  hyperon in  $\Xi$  matter  $U^{(\Xi)} = -55.6\text{MeV}$ . In S271, the same potential is taken to obtain the

ratio  $g_{\sigma^*\Lambda}/g_{\sigma N} = 0.77$ . In this way, the  $\Delta B_{\Lambda\Lambda}$  of  $^{10}_{\Lambda\Lambda}\text{Be}$  is improved from 0.38 MeV to 2.2 MeV in NL3, and from 0.2 MeV to 3.9 MeV in S271, much close to the extracted value  $4 \sim 5$  MeV. The  $g_{\sigma^*\Xi}$  is determined by the  $\Xi$  hyperon potential in  $\Xi$  matter  $U_{\Xi}^{(\Xi)} = -40\text{MeV}$ [19]. The  $\omega NN$  tensor coupling is vanishing, and the  $\omega\Lambda\Lambda$  tensor coupling is small but adjusted to simulate the vanishing spin-orbit splitting for the  $\Lambda$  hyperon observed in  $^{16}_{\Lambda}\text{O}$ .

For simplicity, we perform calculations for various isoscalar-isovector coupling  $\Lambda_v$ 's, and the  $\Lambda_s$  is set as zero. For a given coupling  $\Lambda_v$ , we follow Ref.[6, 8] to readjust the  $\rho NN$  coupling constant  $g_{\rho N}$  so as to keep an average symmetry energy fixed as 25.7 at  $k_F = 1.15 \text{ fm}^{-1}$ . In doing so, it was found in Ref.[6] that the binding energy of  $^{208}\text{Pb}$  is nearly unchanged for various  $\Lambda_v$ 's. Below, we will see how the total binding energy of multi- $\Lambda$  hypernuclei is modified by the  $\Lambda_v$ .

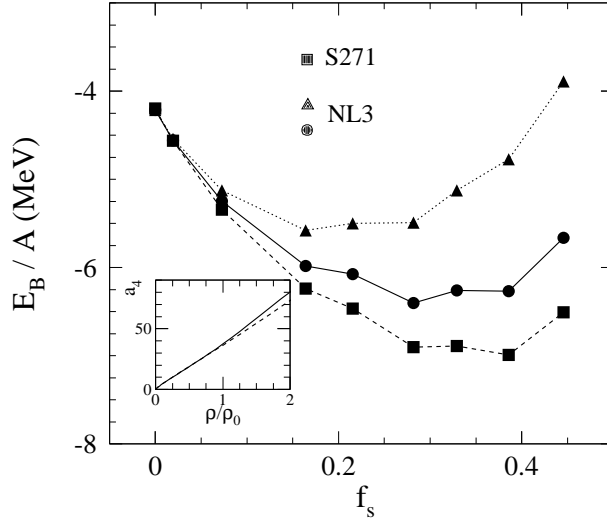


Figure 1: Binding energy per baryon for various  $^{102}\text{Ca}+\Lambda$ 's systems as a function of the strangeness fraction  $f_s = n_{\Lambda}/n_B$  at  $\Lambda_v = 0$ . The symbols from left correspond to the hyperon number 0, 2, 8, 20, 28, 40, 50, 64, and 82, respectively. Except for results marked by the triangles, the strange mesons are considered. The solid and dashed curves in the inset are for the symmetry energy in NL3 and S271, respectively.

The binding energy per baryon for various  $^{102}\text{Ca}+\Lambda$ 's systems is displayed in Fig.1. Metastable minima appears with the rise of the  $\Lambda$  hyperon number  $n_{\Lambda}$ . The additional  $\Lambda\Lambda$  attraction, simulated by the strange mesons, produces much larger binding energy at larger  $f_s$  and shifts the minima outwards. The difference of binding energies of multi- $\Lambda$  hypernuclei

in NL3 and in S271 enlarges explicitly with the rise of  $n_\Lambda$ . Since both models share the same saturation properties and take the same potential for the  $\Lambda$  hyperon, this enlargement is attributed to the different density dependence of the symmetry energy. With the rise of  $n_\Lambda$ , the central density of multi- $\Lambda$  hypernuclei increases. For instance, the central density in  $^{102}\text{Ca}+50\Lambda$  is about  $1.43\rho_0$  in NL3 which is much larger than  $1.06\rho_0$  in  $^{102}\text{Ca}$ . The more different symmetry energy at the larger density domain, shown in the inset in Fig.1, thus accounts for the large difference of the binding energy at larger  $f_s$ .

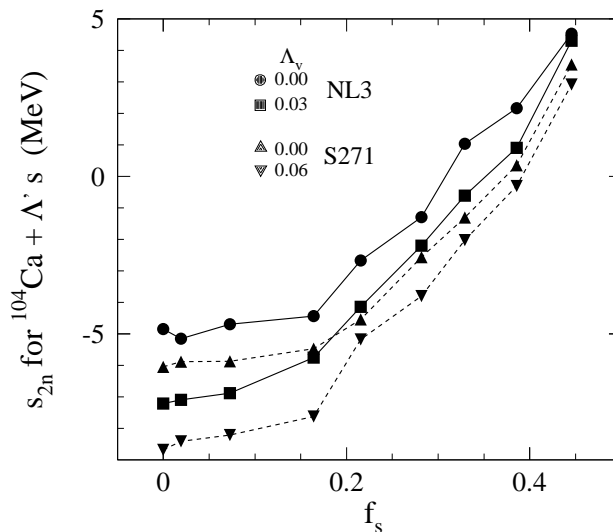


Figure 2: Two-neutron separation energy for  $^{104}\text{Ca}+\Lambda$  systems vs.  $f_s$ .

Fig.2 shows that the two-neutron separation energy of  $^{104}\text{Ca}+\Lambda$ 's systems increases from the negative to the positive with the rise of  $n_\Lambda$ . As the  $n_\Lambda$  increases, the nucleon potential is enhanced by the attraction between hyperons and nucleons, being able to fill in more neutrons under the continuum. The neutron drip line can thus be largely extended. For instance, the drip line of Ca isotope can be extended from the neutron number 50[31] to 82 as long as about 50  $\Lambda$ 's are filled in. The dependence of the separation energy on the isoscalar-isovector coupling  $\Lambda_v$  reduces approximately with the increase of  $n_\Lambda$ . In Refs.[18, 19], a large class of MEMOs are constructed by adding multi-hyperons in stable nuclei, while here we aim at the extension of the neutron drip line by filling in  $\Lambda$  hyperons in unstable isotopes. As multi- $\Lambda$  hypernuclei may exert their roles in extending the neutron drip line and binding

baryons more strongly than in normal nuclei, they will potentially influence the astrophysical nucleosynthesis and the abundances of elements. To search for multi- $\Lambda$  hypernuclei with the  $n_\Lambda$  up to 50 is possible but certainly difficult[20]. Here, we just devote ourselves to investigating the sensitivity of properties of such exotic systems to the density dependence of the symmetry energy.

The sensitivity of the total binding energy to the  $\Lambda_v$  is different for various  $^{102}\text{Ca}+\Lambda$ 's systems. For  $^{102}\text{Ca}+\Lambda$ 's systems that are unstable against the neutron emission at small  $n_\Lambda$  and unstable against the  $\Lambda$  hyperon emission at very large  $n_\Lambda$ , the total binding energies can be modified by as much as tens of MeV for various  $\Lambda_v$ 's. For stable  $^{102}\text{Ca}+\Lambda$ 's systems whose binding energies are situated on or very close to the minima, shown in Fig.1, the modification to the total binding energies by various  $\Lambda_v$ 's is quite small. For instance, the total binding energy for  $^{102}\text{Ca}+50\Lambda$  in NL3 is just modified by up to 2MeV with various  $\Lambda_v$  values.

A data to data correlation of the neutron thicknesses between  $^{208}\text{Pb}$  and stable multi- $\Lambda$  nuclei can be established as in Refs.[8, 10]. The neutron thickness of these stable multi- $\Lambda$  nuclei is very sensitive to the  $\Lambda_v$ . For instance, the uncertainty of the neutron thickness for  $^{102}\text{Ca}+40\Lambda$  and  $^{102}\text{Ca}+50\Lambda$  is about 3 times that for  $^{208}\text{Pb}$ . The proton density distribution in these exotic system is also sensitive to the  $\Lambda_v$  and one third of the uncertainty of the neutron thickness comes from the protons. The large uncertainty of the neutron thickness is attributed to the addition of the  $\Lambda$  hyperons, which will be elucidated below.

Usually, one modifies the isospin dependent potential considering the shift of the isospin and the isovector field directly. Here, we modify it by enhancing the isoscalar field ( $\omega$  field) through filling in  $\Lambda$ 's without changing the isospin of the system, which is fulfilled by considering the isoscalar-isovector coupling. In Fig.3, the isovector potentials are displayed for  $^{102}\text{Ca}$  and  $^{102}\text{Ca}+50\Lambda$  in NL3. In S271, similar results for these two systems can be obtained. The isovector potentials for various  $\Lambda_v$ 's in the exotic isotope are largely shifted by filling in considerable  $\Lambda$  hyperons. The uncertainty of the isovector potential against the  $\Lambda_v$  in  $^{102}\text{Ca}$  is much larger in the larger radius region, compatible with the understanding that  $^{102}\text{Ca}$  is totally diffusive and unstable. Compared to results for  $^{102}\text{Ca}$ , the sensitivity of the isovector potential to the  $\Lambda_v$  in  $^{102}\text{Ca}+50\Lambda$  is shifted to the central region, and at the large radius the convergence occurs, which is favored by the extension of the neutron drip line. The results shown in Fig.3 for two exotic systems are related to different density profiles. The central

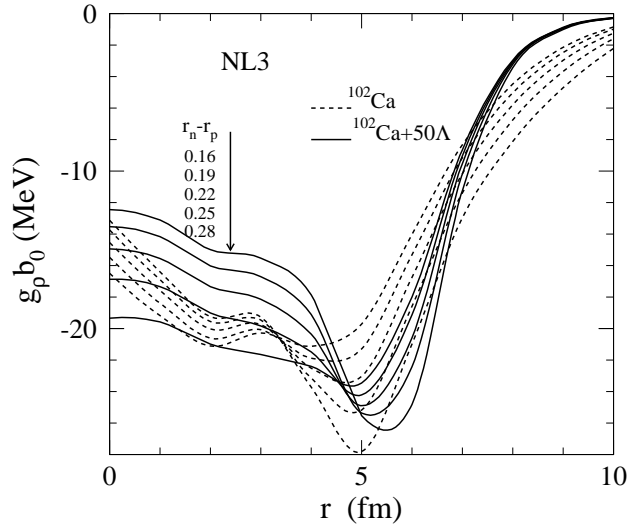


Figure 3: The isovector potential for  $^{102}\text{Ca}$  and  $^{102}\text{Ca}+50\Lambda$  in NL3 vs. radius. The curves from above (near the arrow) are obtained with various  $\Lambda_v$ 's (equally from 0.04 to 0.00) which give the neutron thicknesses (in fm) in  $^{208}\text{Pb}$  as denoted in ascending order.

density in  $^{102}\text{Ca}+50\Lambda$  is about one third higher than that in  $^{102}\text{Ca}$ . The deviation of the symmetry energy for various  $\Lambda_v$ 's enlarges with the rise of the density beyond the normal density or even much lower density [4, 6, 7]. At the central region in  $^{102}\text{Ca}+50\Lambda$ , the isovector potential is more sensitive to the  $\Lambda_v$  than that in  $^{102}\text{Ca}$ . The isoscalar potential can also be shifted to a certain degree by the  $\Lambda_v$ , whereas for the normal nuclei the shift is negligible. The sensitivity of the isovector potential to the  $\Lambda_v$  is responsible for the uncertainty of the neutron thickness.

The  $\Lambda$  hyperon constituent is important in astrophysical bulk matter to explore the effects of the density dependence of the symmetry energy. We plot the  $\Lambda$  and  $\Xi^-$  fractions defined by  $f_Y = \rho_Y / \rho_B$  in Fig.4 with the S271 based on a self-consistent calculation. The large sensitivity of the hyperon fractions to the  $\Lambda_v$  occurs at about  $2 \sim 3\rho_0$  where the  $\Lambda$  hyperon starts to appear. Since the density as high as  $2 \sim 3\rho_0$  is accessible through the heavy ion collisions with the colliding energy about 1GeV per nucleon, the detection related to the hyperons, especially the  $\Lambda$ 's, in heavy ion collisions is helpful to probe the density dependence of the nuclear symmetry energy. The starting density for the  $\Lambda$  appearance is model dependent. For instance, it is about  $1.8\rho_0$  in NL3 and  $2.2\rho_0$  in S271. As shown in the inset in Fig.4, a shift

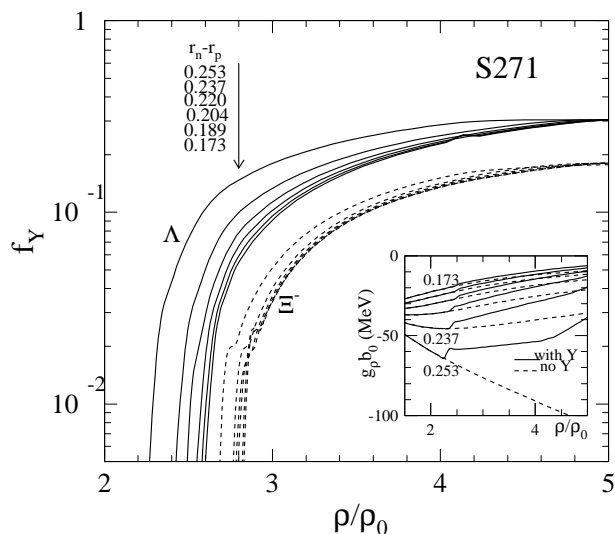


Figure 4: Hyperon fractions in S271 vs. baryon density in hyperon-rich matter. The curves from above are for different values of  $\Lambda_v$  (equally from 0.00 to 0.05) that give the neutron thicknesses in  $^{208}\text{Pb}$  as denoted in descending order. The inset shows the isovector potential with hyperons and without.

of the isovector potential starts to appear with the  $\Lambda$  appearance, and the isovector potential differs more from that without hyperonization with the increase of the density. In multi- $\Lambda$  nuclei far from the normal drip line, the isovector potential is shifted by filling in  $\Lambda$ 's under the fixed isospin, while here the shift comes from the change of the isospin and the isoscalar field together. The convergent extent with respect to the  $\Lambda_v$  exists for the hyperon fraction in the whole density domain. This indicates that it is favorable to include the isoscalar-isovector coupling terms for the model itself. At very high densities, the convergence of hyperon fractions occurs. This is attributed to the fact that the isospin is largely suppressed with the drop of the neutron fraction at high densities. The isovector potential is thus small compared to the isoscalar potential, so that the isoscalar potential is little changed through the isoscalar-isovector coupling. This implies that the hyperstars[24] whose core is solely composed of hypermatter at high densities will be insensitive to the  $\Lambda_v$ .

The large reduction of the maximum mass of neutron stars by hyperonization, firstly pointed out by Glendenning (see Ref.[21] and references therein), can be reproduced here. In NL3, hyperonization in the core reduces the maximum neutron star mass by about  $0.9M_\odot$

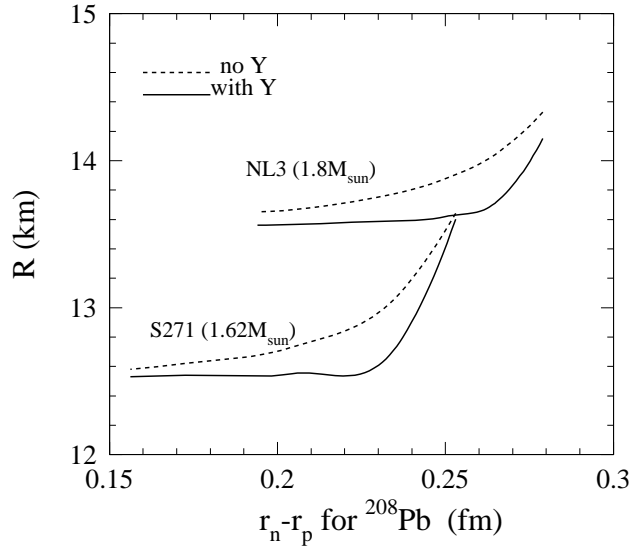


Figure 5: Radii of neutron stars as a function of the neutron thickness in  $^{208}\text{Pb}$ .

from about  $2.8M_{\odot}$ , and by  $0.75M_{\odot}$  from about  $2.4M_{\odot}$  in S271. Compared to models in which hyperons are absent, hyperonization in the neutron star whose mass is near the maximum mass increases the central baryon density by as much as  $1\rho_0$  in the region  $r < 5\text{km}$ . For a  $1.4$  solar-mass neutron star, the role of hyperonization is quite limited because of relative low core densities. Using the Oppenheimer-Volkoff equations for bulk matter in beta equilibrium, we thus investigate neutron stars with relative large masses:  $1.8M_{\odot}$  with the NL3 model and  $1.62M_{\odot}$  with the S271 model. In Fig.5, the radii of neutron stars with respective masses in two models are displayed as a function of the neutron thickness for  $^{208}\text{Pb}$ . The radius  $R$  of neutron star without hyperonization increases with the neutron thickness in  $^{208}\text{Pb}$  for a given parameter set, which is the same as in Ref.[7]. For neutron stars with hyperonization, the trend is similar, whereas the correlation between the  $R$  and the neutron thickness in  $^{208}\text{Pb}$  almost vanishes in a large region of the neutron thickness in  $^{208}\text{Pb}$ . This property is consistent with the convergent extent shown in Fig.4. It indicates that for a neutron star with hyperonization the radius  $R$  nearly just depends on the on-off switch rather than concrete values of the isoscalar-isovector coupling in a given model. An accurate measurement of the neutron radius for  $^{208}\text{Pb}$  at the Jefferson Laboratory[32] determines the density dependence of the symmetry energy at low densities, as pointed out in Ref.[7]. The measurement of

the radius of the neutron star with hyperonization can discriminate two regions of the  $\Lambda_v$ 's to which the R is either very sensitive or insensitive at high densities. Various information through separate measurements may be combined together to constrain the isoscalar-isovector coupling that modifies the density dependence of the symmetry energy in the whole density region.

In summary, we have studied the roles of the isoscalar  $\Lambda$  hyperons in exploring the density dependence of the symmetry energy in multi- $\Lambda$  hypernuclei, hyperon-rich matter and neutron stars with RMF models. Relationships between the properties of three types of objects and the neutron thickness in  $^{208}\text{Pb}$  are established with respect to the isoscalar-isovector coupling that modifies the density dependence of the symmetry energy. The exotic isotopes far from the neutron drip line can be stabilized by filling in considerable  $\Lambda$  hyperons, and the neutron drip line is substantially extended outwards. The difference of the binding energy of multi- $\Lambda$  hypernuclei from different models is attributed to different symmetry energies. The isovector potential together with the neutron thickness in multi- $\Lambda$  hypernuclei situated on the new drip line that is far from the normal drip line is very sensitive to the isoscalar-isovector coupling. In beta equilibrated hyperon-rich matter, we have investigated the sensitivity of the hyperon fractions to the isoscalar-isovector coupling based on the self-consistent calculation for hyperons and nucleons. The large sensitivity of the  $\Lambda$  hyperon fraction to the isoscalar-isovector coupling occurs at about  $2 \sim 3\rho_0$ . The properties of neutron stars are investigated. An on-off effect with respect to the isoscalar-isovector coupling exists for the radius of neutron stars with hyperonization. Besides the detection of  $\Lambda$  hyperons in the heavy ion collisions, the measurements of the neutron star radius and neutron thickness in  $^{208}\text{Pb}$  could help set up the constraints on the density dependence of the symmetry energy.

## Acknowledgement

This work is partially supported by the National Natural Sciences Foundation of China under grant No.10405031. The author thanks Prof. M. Di Toro for helpful discussions.

## References

- [1] H. A. Bethe, Rev. Mod. Phys. 62, 801 (1990)

- [2] I. Bombaci, in *Isospin Physics in Heavy-Ion Collisions at Intermediate Energies*, edited by B.A.Li and W. Udo Schröder (Nova Science Publishers, Inc., New York, 2001), p35
- [3] A.W. Steiner, M. Prakash, J.M. Lattimer, P.J. Ellis, *Phys. Rept.* 411 (2005) 325
- [4] B.A.Brown, *Phys. Rev. Lett.* 85(2000)5296
- [5] B.A.Li, *Phys. Rev. Lett.* 85(2000)4221; *ibid.*88(2002)192701
- [6] C.J.Horowitz, J.Piekarewicz, *Phys. Rev. Lett.*86(2001)5647
- [7] C.J.Horowitz, J.Piekarewicz, *Phys. Rev. C*64(2001)062802(R); *ibid.*,C66(2002)055803
- [8] B.G.Todd, J.Piekarewicz, *Phys. Rev. C*67(2003)044317
- [9] Y.B. Wei Y.G. Ma W.Q. Shen, et.al. *Phys.Lett.*B586(2004)225
- [10] W.Z.Jiang, Y.L.Zhao, *Phys. Lett.* B617(2005)33
- [11] L.W.Chen, V.Greco, C.M.Ko, B.A. Li, *Phys. Rev. Lett.* 90(2003)162701
- [12] M. Di Toro, A. Drago, T. Gaitanos, V. Greco, A. Lavagno, *nucl-th/0602052*
- [13] J.Carriere, C.J.Horowitz, J.Piekarewicz, *Astrophys. J* 593(2003)463
- [14] W.Z.Jiang, Y.L.Zhao, Z.Y.Zhu, S.F.Shen, *Phys. Rev. C*72 (2005)024313
- [15] S.Aoki, et al *Prog. Theor. Phys.* 85(1991)1287
- [16] J.K.Ahn, et al *Phys. Rev. Lett.* 87(2001)132504
- [17] J.K.Takahashi, et al *Phys. Rev. Lett.* 87(2001)212502
- [18] J.Schaffner, C. B.Dover, A.Gal, C.Greiner, H.Stöcker, *Phys. Rev. Lett.* 71(1993)1328
- [19] J.Schaffner, C.B.Dover, A.Gal, C.Greiner, D.J. Millener, and H.Stöcker, *Ann. Phys.* (N.Y.) 235 (1994) 35
- [20] D.Javorsek II, E.Fischbach and D.Elmore,*Phys. Rev.* D67(2003)034015
- [21] N.K.Glendenning, *Phys.Rept.*342(2001)393
- [22] N.K. Glendenning, *Astrophys. J.* 293 (1985) 470

- [23] N.K. Glendenning, S.A. Moszkowski, Phys. Rev. Lett. 67 (1991) 2414
- [24] J.Schaffner-Bielich, M.Hanuske, H.Stöcker, W.Greiner, Phys. Rev. Lett. 89(2002)171101
- [25] J.Schaffner-Bielich, A.Gal, Phys. Rev. C62(2000)034311
- [26] M.Prakash, I.Bombaci, M.Prakasha, P.J. Ellis, J.M. Lattimer and R.Knorren, Phys. Rept. 280(1997)1
- [27] J.Mares,E.Friedman, A.Gal, and B.K.Jennings, Nucl. Phys. A594(1995)311
- [28] B.D.Serot, J.D.Walecka, Adv. Nucl. Phys. 16(1986)1; Int.J.Mod.Phys. E6(1997)515
- [29] P.Ring, Prog. Part. Nucl. Phys. 37(1996)193
- [30] G.A.Lalazissis, J.König, P.Ring, Phys. Rev. C55(1997)540
- [31] J.Meng, H. Toki, J.Y.Zeng, S.Q.Zhang, and S.G.Zhou, Phys. Rev. C 65 (2002) 041302(R)
- [32] R.Michaels, P.A.Souder, G.M.Urciuoli, spokespersons, Jefferson Laboratory Experiment E-00-003